



Original Research

Revealing the role of microalgae-bacteria niche for boosting wastewater treatment and energy reclamation in response to temperature



Chaofan Zhang^{a,1}, Xi Chen^{a,1}, Meina Han^a, Xue Li^a, Haixing Chang^b, Nanqi Ren^a, Shih-Hsin Ho^{a,*}

^a State Key Laboratory of Urban Water Resource and Environment, School of Environment, Harbin Institute of Technology, Harbin, 150090, PR China

^b School of Chemistry and Chemical Engineering, Chongqing University of Technology, Chongqing, 400054, PR China

ARTICLE INFO

Article history:

Received 20 August 2022

Received in revised form

30 November 2022

Accepted 1 December 2022

Keywords:

Metabolomics

Niche width

Pathogens

Nutrients removal

Microbial community assembly

ABSTRACT

Conventional biological treatment usually cannot achieve the same high water quality as advanced treatment when conducted under varied temperatures. Here, satisfactory wastewater treatment efficiency was observed in a microalgae-bacteria consortia (MBC) over a wide temperature range because of the predominance of microalgae. Microalgae contributed more toward wastewater treatment at low temperature because of the unsatisfactory performance of the accompanying bacteria, which experienced cold stress (e.g., bacterial abundance below 3000 sequences) and executed defensive strategies (e.g., enrichment of cold-shock proteins). A low abundance of *amoA-C* and *hao* indicated that conventional nitrogen removal was replaced through the involvement of microalgae. Diverse heterotrophic bacteria for nitrogen removal were identified at medium and high temperatures, implying this microbial niche treatment contained diverse flexible consortia with temperature variation. Additionally, pathogenic bacteria were eliminated through microalgal photosynthesis. After fitting the neutral community model and calculating the ecological niche, microalgae achieved a maximum niche breadth of 5.21 and the lowest niche overlap of 0.38, while the accompanying bacterial community in the consortia were shaped through deterministic processes. Finally, the maximum energy yield of 87.4 kJ L⁻¹ and lipid production of 1.9 g L⁻¹ were achieved at medium temperature. Altogether, this study demonstrates that advanced treatment and energy reclamation can be achieved through microalgae-bacteria niche strategies.

© 2022 Published by Elsevier B.V. on behalf of Chinese Society for Environmental Sciences, Harbin Institute of Technology, Chinese Research Academy of Environmental Sciences. This is an open access article under the CC BY-NC-ND license (<http://creativecommons.org/licenses/by-nc-nd/4.0/>).

1. Introduction

Recently, the attention to wastewater treatment has shifted from satisfactory efficiency to achieving both water purification and resource recovery. The growing requirements of the urban population mean that a large amount (330 km³) of municipal wastewater is generated worldwide annually [1]. Current wastewater management still has challenges, such as advanced nutrient removal, emerging pollutant control, and limited reclamation options [2]. An estimated 80% of the effluents discharged into the

aquatic environment still pose various risks or concerns [3]. Microalgae-based wastewater treatment provides a promising alternative because of its great prospects for carbon neutrality, advanced treatment, and bioenergy production [4,5]. A wide range of microalgae wastewater treatment systems have been developed for large-scale applications, including open systems, closed systems, and biofilm systems [6]. Moreover, coupling microalgae with bacteria for wastewater treatment usually had better efficiency and more stable performance for nutrient removal [7].

The structure and dynamics of the microbial community could directly influence the process performance and stability during biological wastewater treatment. When rational interaction and functional biodiversity are developed in the microbial community, treatment efficacy and function will improve [8]. In natural aquatic ecosystems, phototrophic/mixotrophic microalgae and bacteria

* Corresponding author.

E-mail addresses: stephen6949@hit.edu.cn, stephen6949@msn.com (S.-H. Ho).

¹ These authors contributed equally to this work.

predominantly occupy the producer and decomposer roles, respectively, suggesting their different features may be employed to maintain water quality and ecological balance [9]. Thus, microalgae-bacteria wastewater treatment carried out by diverse microbial niches may be an important way to achieve the desired system performance.

Additionally, the effluents from conventional biological processes do not satisfy the increasingly stringent standards for nutrient discharge and can induce eutrophication in receiving water bodies [10]. One key reason is that removing nitrogen (N) and phosphorus (P) requires specific functional bacteria. For instance, nitrogen is conventionally removed through two consecutive processes: nitrification and denitrification [8]; *Nitrosococcus* sp., *Nitrosomonas* sp., *Nitrosospira* sp., *Alcligenes* sp., and *Paracoccus* sp., are widely known as nitrifying and denitrifying strains [11]. Phosphorus is removed via polyphosphate-accumulating microorganisms (PAOs) and glycogen-accumulating organisms (GAOs) [12]. However, the habitats of these functional bacteria require different redox conditions. For instance, the chemoautotrophic ammonia-oxidizing archaea, chemoautotrophic ammonium-oxidizing bacteria, and chemoautotrophic nitrite-oxidizing bacteria grow under aerobic conditions, but heterotrophic denitrifying bacteria (DNB), PAOs, and GAOs thrive within an anoxic/anaerobic environment [13]. In addition, the solid retention time of the above strains and the slow growth rate of chemoautotrophic bacteria may discourage the practical operation of these reactors while also considering temperature variation [11]. In contrast, satisfactory outcomes could be achieved via a microalgae-bacteria system under a wide range of temperatures without maintaining the specific redox conditions [14,15]. Despite the promise of this strategy, a systematic study of nutrient removal via microalgae-bacteria consortia (MBC) from the perspective of ecological niches in response to different temperature profiles has not been done.

In this study, the microalgae *Chlamydomonas* sp. JSC₄ was selected for examination owing to its high growth rate, superior environmental tolerance, and satisfactory bioenergy potential [16]. Three temperature conditions were used to comprehensively investigate the relationships in the MBC. The correlation between MBC treatment efficacy and the temperature was assessed through nutrient removal, structural equation models, and Arrhenius plot-fitting after non-metric multidimensional scaling (NMDS) and ternary analysis. Next, the alterations in the microbial community and functional metabolic profiles were analyzed using an UpSet plot, PICRUSt interpretation, photosynthetic function, and metabolomics. The changes in the accompanying bacterial communities were examined through calculations of the neutral community model, niche breadth, and niche overlap. Finally, the potential for biodiesel production and energy yield from this symbiotic system was evaluated. Overall, this study aims to better understand the role of the microalgae-bacteria niche for wastewater treatment, accelerating its applicability for both advanced treatment and resource reclamation.

2. Materials and methods

2.1. Cultivation of MBC and experimental set-up

Chlamydomonas sp. JSC₄ (NCBI: KF383270) was pre-cultivated in modified Bold 3 N medium, aerating at 2% CO₂, and illuminating with 150 $\mu\text{mol m}^{-2} \text{s}^{-1}$ for six days, as previously reported [16]. Municipal wastewater obtained from a local wastewater treatment plant (WWTP) in Harbin, China, was used for the subsequent experiments after filtration through a 0.45 μm membrane; the wastewater parameters were determined as: chemical oxygen demand (COD) = 248.147 mg O₂ L⁻¹, total nitrogen

(TN) = 64.59 mg L⁻¹, and total phosphorus (TP) = 11.18 mg L⁻¹. Finally, 80 mg L⁻¹ of strain JSC₄ was inoculated into a 1 L batch photobioreactor and cultivated at 300 rpm stirring, 200 $\mu\text{mol m}^{-2} \text{s}^{-1}$ irradiance, and 2% CO₂ feeding at 20, 30, and 40 °C (hydraulic retention time = 6 days). All treatments were carried out in triplicate.

2.2. Analytical methods

COD, TP, and TN were measured by potassium dichromate-sulfuric acid digestion, ammonium molybdate spectrophotometry, and alkaline persulfate digestion, respectively [17]. Microalgal growth was determined by measuring the optical density at 682 nm wavelength (OD₆₈₂) using a UV/VIS spectrophotometer (UVmini-1240, Shimadzu, Tokyo, Japan) with a conversion factor of 1.0 OD₆₈₂ = 0.8 g L⁻¹ biomass. Lipid content, production, and composition of lyophilized microalgae were determined through direct transesterification and gas chromatography-mass spectrometry (GC/MS, GCMS-QP2010 Plus, Shimadzu, Japan) as previously reported [18]. Biodiesel quality and energy yield potential were calculated by empirical equations as previously reported [18,19]. The photochemical parameter (F_v/F_m) was directly acquired using an AquaPen fluorometer (AP-C 100, PSI, Czech Republic). As previously reported, Carbohydrate concentration was determined using the colorimetric method with anthrone reagents [18]. The detailed pretreatment and calculation methods related to lipid and carbohydrate determination are displayed in Text S1. The proline concentration was determined using the Proline Content Assay Kit (catalog number AKAM003C, Boxbio Science & Technology Co., Ltd., Beijing).

2.3. Analysis of bacterial community and microalgal metabolic profiling

The bacterial community was investigated through 16S rDNA amplicon sequencing. DNA extraction and data analysis were done as previously reported, including sequencing, data analysis, operational taxonomic unit (OTU) clustering, species annotation, and alpha diversity analysis; these details are described in Text S2. Functional analysis was analyzed from the 16S rRNA gene-based microbial compositions using the PICRUSt algorithm established on the Kyoto Encyclopedia of Gene and Genomes (KEGG). Metabolic profiling analysis was determined using capillary electrophoresis/mass spectrometry, adopting the Agilent G6224AA LC/MSD time-of-flight system alongside the auxiliary MassHunter software as previously reported [16]; details can be found in Text S3.

Corresponding conditions were characterized, and analyses were performed to further reveal the relationship between the microalgae and bacterial community. The similarities between different groups were first described by correlation coefficients based on the Spearman calculation. Samples from the same temperatures were then combined into one group to evaluate the influence of temperature variation on the microbial community through NMDS. Groups at the species level were collected to screen enriched species using ternary phase diagrams after the log₂ transformation of data. The enriched species were divided into three clusters based on the temperature conditions of their growth. Finally, the correlations among wastewater treatment efficacy, characterization of the bacterial community, and growth status of microalgae were evaluated by structural equation models (AMOS 21.0, IBM Corporation Software Group, USA). Arrhenius plots were established using $\ln(k)$ against $1/T$, where k is the growth status (OTU abundance), and T is the absolute temperature [20].

The global co-occurrence patterns of the microbial community were elicited through network analysis. The topology results of the

network were calculated using the *igraph* package in R (Version 3.6.2). Species with positive correlations were further screened and clustered by modularity analysis using *Gephi* (Version 0.9.2). The contribution of the stochastic process to microbial community assembly was determined by the neutral community model using least squares regression [21]. The analysis of niche breadth and niche overlap were carried out based on the predominant clustered interacting microbial community. The niche breadth and niche overlap of the microbial community were determined with the Levins' index using the *spaa* package in R (Version 3.6.2); the detailed formulas for these analyses are described in Text S4 [22].

2.4. Statistical analysis and data visualization

The pathways comparisons among low-, medium-, and high-temperature groups were visualized with Welch's tests using *STAMP* (Version 2.1.3). Heatmaps (*pheatmap* package and *stats* package), Sankey diagrams (*ggalluvial* package), Venn diagram (*VennDiagram* package), and UpSet plots (*UpSetR* package and *yyplot* package) were generated using the corresponding packages in R (Version 3.6.2). The correlation analysis was calculated using the *psych* package in R (Version 3.6.2); all data for bioinformatics analysis were tested by the Tukey test and Wilcoxon test. A network map was established based on the Spearman's rank correlations with a screening parameter of $r > 0.8$ and a P -value < 0.01 between two items.

3. Results and discussion

3.1. Relationship between treatment efficiency and temperature during MBC treatment

3.1.1. Efficiency and characterization of wastewater treatment by MBC

The desirable performance of wastewater treatment was achieved by MBC for all conditions, and the optimal temperature condition was found to be the medium temperature (Fig. 1a–c). The average value of residual COD was $\sim 50 \text{ mg L}^{-1}$ on day 4, which is in accordance with the Class I discharge standard in China (Fig. 1a). Regardless of temperature variation, COD and TP were completely removed on day 5 and day 2, respectively (Fig. 1a and b). The quick removal of COD and P before nitrogen removal indicated that MBC could involve an exclusive removal mechanism, which does not occur in activated sludge treatment [10,23]. Inorganic phosphorus could be directly assimilated by microalgae through phosphorylation, then promptly biosynthesized into adenosine triphosphate (ATP) and nicotinamide adenine dinucleotide phosphate oxidase (NADPH) [8]. Therefore, the superior TP removal by MBC could be mainly attributed to microalgae. Similarly, on day 4, 100% TN removal was achieved at medium and high temperatures, while the residual TN at low temperature was only $\sim 14 \text{ mg L}^{-1}$ (Fig. 1c), which also satisfies the Class I discharge standard in China. TN was often instantly removed at the same high efficiency as previous activated sludge treatment [12,23]. However, unlike previous reports, the TN removal rate gradually decreased during the treatment period, implying that the involvement of microalgae might alter the elimination pathway of TN. Therefore, the characterization of functional features and the alterations to the microbial community in this biological system should be comprehensively scrutinized.

The microalgal biomass was almost equivalent on day 2 at low temperature (2 g L^{-1}) and medium temperature (2.1 g L^{-1}) (Fig. 1d). In contrast, on day 2, the abundance of bacterial communities (< 3000 sequences) at low temperature was approximately 95% lower than at medium temperature (> 50000 sequences) and 92.5% lower than at high temperature (> 40000 sequences) (Fig. 1e). The

distinctly different growth tendencies of eukaryotic microalgae and prokaryotic bacteria suggest that microalgae could contribute more to COD elimination at low temperature. Overall, the microalgal species in this study were more suitable for decentralized wastewater applications because the time for COD removal was longer. Additionally, the predominant bacterial species were different for each condition (Fig. 1e). *Chryseobacterium indologenes* (Label-2 in Fig. 1e) were dominant at low temperature, while *Bacillus cohnii* (Label-1 in Fig. 1e) and *Ralstonia pickettii* (Label-3 in Fig. 1e) were the dominant species at high temperature. Therefore, the temperature was an important factor for the different symbiotic relationships between microalgae and bacteria, also suggesting that related functions might be altered at different temperatures.

The microalgal biomass was enhanced until day 6 of the experiment (Fig. S1), and the microbial community abundance was strongly decreased (Fig. 1e), indicating that the eukaryotic microalgae and prokaryotic bacteria might have separate roles during treatment. The alpha diversity indices varied significantly across the samples, demonstrating that the structural differences in the microbial community were affected by different temperatures (Table S1). Additionally, the alpha diversity indices were lower than those commonly found in municipal-activated sludge treatment systems [22,24]. For instance, the Shannon index in this experiment was only 1.6–2.9 (Table S1), indicating that some specific functional or accompanying bacteria were enriched with microalgal growth.

3.1.2. Relationship between treatment efficiency and MBC

Analogous to the alpha diversity results, the similarity examination based on Spearman correlation also indicated that the species composition significantly differed among samples (Fig. S2). Furthermore, the NMDS analysis based on Bray-Curtis calculations further confirmed the difference among the species compositions (stress value = 0.0001) when the samples were divided by different temperature conditions (Fig. 2a). The core microbial species at low-, medium-, and high-temperature conditions were further screened by a ternary plot (Fig. 2b) and assigned as Cluster I, Cluster II, and Cluster III, respectively (Table S2). To explore this treatment system, structural equation models were further adopted to dissect the relationship between microbial activity and wastewater treatment efficacy at different temperatures [25].

In terms of microbial activity, temperature alteration was negatively associated with the core microbes (Cluster I) under low temperature (blue line with a value of -0.66). The positive correlation of core microbes (Cluster II) at medium temperature (red line with a value of 0.74) was significantly higher than (Cluster III) at high temperature (red line with a value of 0.37) (Fig. 2c). Comparatively, a non-significant relationship was observed for microalgae (gray line with a value of 0.05), further confirming that microalgae were better able to grow than bacteria under low temperature. Furthermore, as the Arrhenius equation manifested, the growth status of microalgae under different temperatures was superior to that of bacteria (Fig. 2d). This indicates that the involvement of microalgae could improve the stability of wastewater treatment when considering low-temperature and temperature-variable systems.

For treatment efficiency, microalgae obviously contributed toward COD removal (red line with a value of 0.89) (Fig. 2c), which indicated the biodegradation of organic pollutants. The cellular size of *Chlamydomonas* sp. JSC₄ is larger than $15 \mu\text{m}$ [18], implying that additional biological functions like endocytosis and binding protein-dependent transport could promote treatment efficiency [26]. Therefore, to improve the performance of wastewater treatment by MBC, a careful selection of a microalgal strain with the potential for assimilating organic matter could be important [27]. Comparatively, the biological functions of the bacterial community

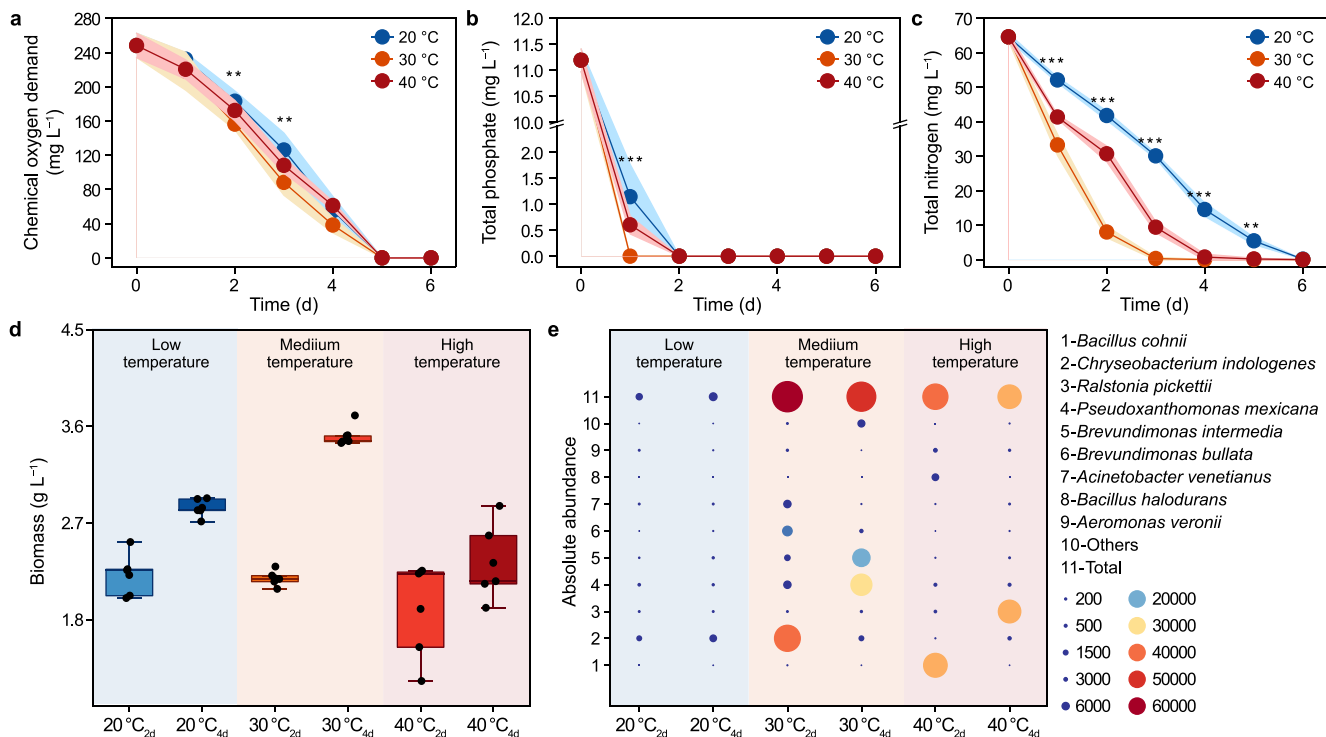


Fig. 1. a–c, Effect of temperatures on COD removal (a), TP removal (b), and TN removal (c) by MBC treatment. d–e, Effect of temperatures on microalgal biomass (d) and the abundance of the core microbial community (e) on day 2 and day 4.

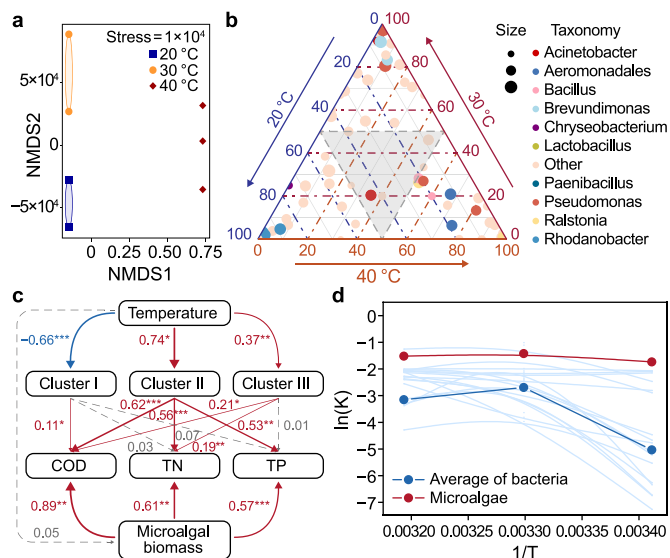


Fig. 2. a, Non-metric multidimensional scaling analysis of the bacterial community under different temperature conditions. b, Ternary plot at the order level using phylogenetic data in response to different temperatures. c, Effect of temperature on microbial activity and wastewater treatment efficiency based on structural equation models. d, Arrhenius plot of the relationship between growth status of microalgae and bacteria and temperature. The numbers below indices indicated the standardized path coefficients. * $P < 0.05$, ** $P < 0.01$, and *** $P < 0.001$. Gray, blue, and red lines represent non-significant, negative, and positive relationships, respectively.

were remarkably varied and were influenced by temperature, as indicated by treatment efficacy. For instance, the core microbes (Cluster II) at medium temperature had a high capacity for the removal of COD (red line with a value of 0.62), TN (red line with a

value of 0.56), and TP (red line with a value of 0.53) (Fig. 2c). In comparison, the core microbes (Cluster I) at low temperature only contributed to COD removal (red line with a value of 0.11), further confirming that temperature was a critical element to alter the bacterial functions. Consequently, MBC may have more endurance and resilience to meet wastewater treatment requirements.

3.2. Alterations of microbial community and functional metabolism

3.2.1. Flexible countermeasure responses to medium and high temperature

Variations in the microbial community and biological functions were scrutinized to disclose the relationship between microalgae and bacteria. At the class level, the microbial community could be divided into four taxa: Alphaproteobacteria (20%), Bacilli (24%), Bacteroidia (20%), and Gammaproteobacteria (36%) (Fig. 3a), which are principally heterotrophic bacteria under aerobic conditions [28]. Surprisingly, the common genera known for nutrient removals, such as *Accumulibacter Candidatus*, *Nitrosomonas* sp., *Nitrobacter* sp., and *Nitrospira* sp. [29], were absent, suggesting a new pattern of nitrogen and phosphate removal. Notably, Caulobacteraceae sp. and Burkholderiales sp. can remove nitrogen via heterotrophic nitrification [30] and heterotrophic denitrification [31] under aerobic conditions, respectively, indicating that nitrogen removal might be achieved through straightforward aerobic processes when microalgae are involved. Weeksellaceae sp. were also detected at medium temperature (Fig. 3a); these are widely deemed as potential pathogens [32]. Xanthomonadaceae are frequently found on fouled membranes because of their function in secreting extracellular polymeric substances [28]. The predominant organisms shifted from Weeksellaceae (73% on day 2) to Xanthomonadaeae (51% on day 4), indicating that the involvement of microalgae could facilitate the elimination of pathogenic bacteria. This shift also indicated that an intimate interaction between

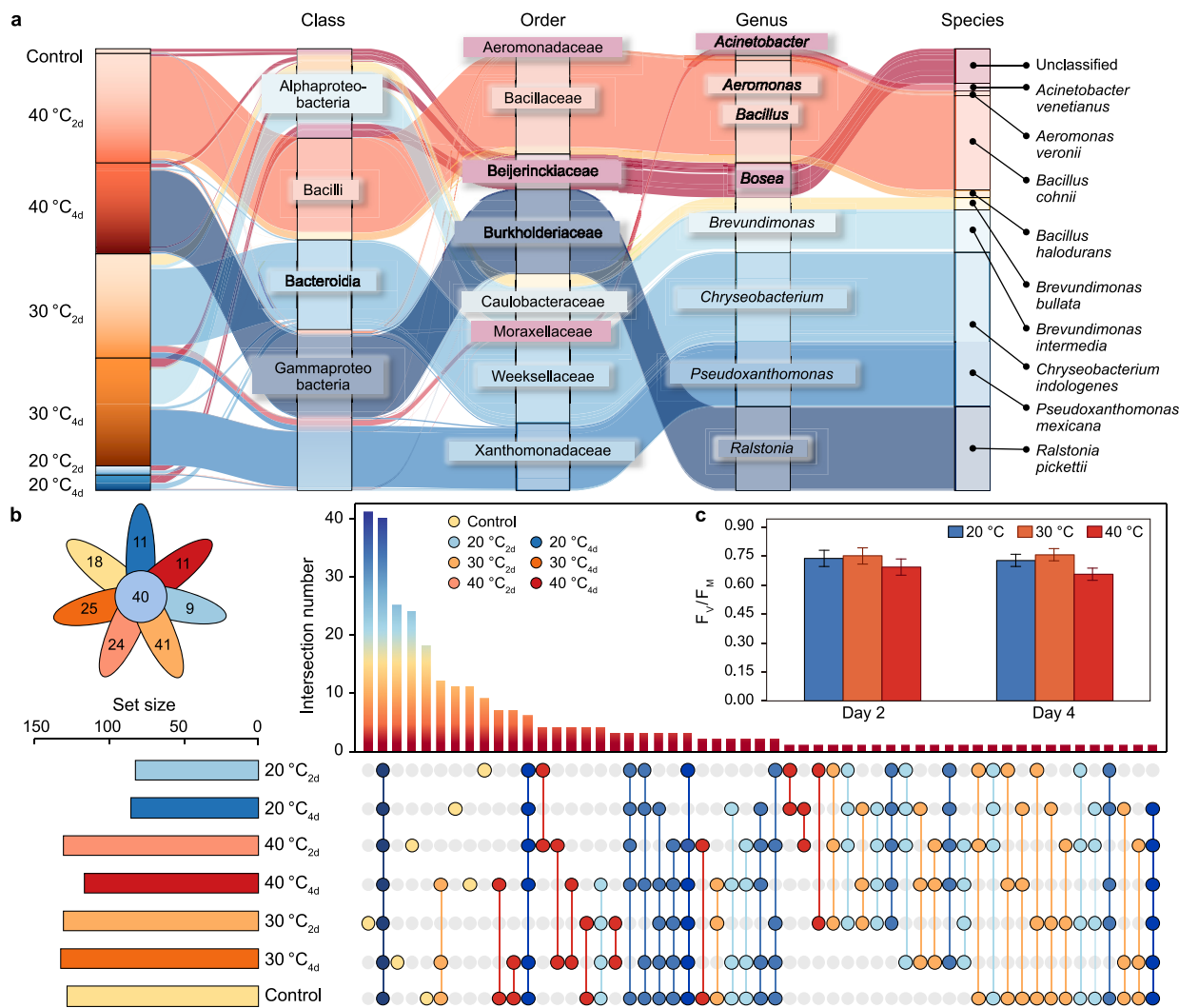


Fig. 3. a, Succession diagram based on the relative abundance of enriched microorganisms at different temperatures on days 2 and 4 using a Sankey plot (at class, order, genus, and species level). b, The total overlap of the number of microorganisms at different temperatures on days 2 and 4 using UpSet and Venn plots at the species level. c, Chlorophyll fluorescence parameters of microalgae at different temperatures on days 2 and 4.

microalgae and bacteria could develop through the compact aggregated microbial flocs. Therefore, MBC could be used to achieve some of these specific biological functions through this superior ecologic phenomenon.

At the species level, the changes in the microbial community were evaluated through UpSet and Venn plots. The non-intersecting objects and intersecting objects are exhibited as gray dots, and colored dots, respectively, and the intersecting objects are interlinked via point lines (Fig. 3b). On day 2, there were 41 non-intersecting objects and 86 intersecting objects at medium temperature (Fig. 3b), indicating a vigorous microbial community. The number of specific strains (non-intersecting objects) reached a maximum at medium temperature, indicating that this temperature was the most favorable condition for both specific and general bacteria to execute their biological functions. Comparatively, for high temperature, there were 24 non-intersecting objects and 119 intersecting objects on day 2 (Fig. 3b), suggesting the microbial community developed a distinct structure at the species level because of the influence of temperature.

Specifically, at medium temperature, the dominant species shifted from *C. indologenes* (61%) to *Pseudoxanthomonas mexicana*

(44%) and *Brevundimonas intermedia* (30%) (Fig. 3a and S3). *C. indologenes* is an antibiotic-resistant pathogenic species found in hospital sewage effluents [33] that primarily biodegrades organic pollutants [34]. *P. mexicana* and *B. intermedia* can heterotrophically remove carbon [35] and aerobically remove nitrogen [36], respectively. Here, microalgal photosynthesis could elevate the oxygen level in wastewater (Fig. 3c), eliminating pathogenic bacteria and generating an aerobic environment [37,38]. The observed transition of dominant species indicated that a desirable performance without the risk of pathogens could be accomplished through this innovative treatment. However, at high temperature, different regulation was observed compared with that observed at medium temperature, where the dominant species changed from *B. cohnii* (75% on day 2) to *R. pickettii* (64% on day 4) (Fig. 3a and S3). Interestingly, *B. cohnii* and *R. pickettii* are commonly seen to remove organic pollutants [39] and nitrogen [40,41] under heterotrophic and aerobic environments. Therefore, similar biological functions, such as the heterotrophic removal of carbon and nitrogen, could be achieved by different dominant species at different temperatures, implying that flexible scenarios could be available for MBC treatment.

3.2.2. Bacterial defensive status and microalgal roles at low temperature

At low temperature, the bacterial community was significantly different from the medium- and high-temperature communities (Fig. 3a). To dissect the response mechanisms at low temperature, the typical metabolic pathways and key functional genes were predicted by PICRUSt based on the KEGG database. Generally, the crucial pathways associated with membrane transport, carbohydrate metabolism, amino acid metabolism, and lipid metabolism were enriched (blue), whereas the signaling molecule interactions, enzyme family activities, and nucleic acid ribosome translation were downregulated (red) (Fig. 4a), representing a characterized cold stress response of the bacterial community [42,43]. DNA repair proteins [44] and DNA gyrase [45] are pivotal components that restore DNA damage induced by cold stress. Here, eight genes (*alkB*, *rmuC*, *radC*, *recO*, *recN*, and *radA* encoding DNA repair proteins; *gryA-B* encoding DNA gyrase) were highly upregulated at low temperature (Fig. 4b and Table S3), indicating the corresponding bacteria were defensively resisting cold stress. Nine other genes (*holA*, *dnaX*, *dinG*, *recQ*, *dnaB*, *recG*, *ruvA-B*, and *rep*) encoding two enzymes (DNA helicase (EC:3.6.4.12) and DNA polymerase (EC:2.7.7.7)) were significantly increased (Fig. 4b and Table S3) as the microbial community attempted to sustain DNA expression. This defensive status could be the principal cause of inhibition of the bacterial community at low temperature (Fig. 1e).

As expected, the abundance of four genes (*cspA*, *pspA*, and *pspC-D*) encoding cold-shock proteins (Fig. 4b and Table S3) were elevated to accommodate cellular metabolism [46]. Additionally,

because cold can trigger reactive oxygen species generation through oxidative stress [47], the abundances of genes (*SOD1-2*, *catG*, *catE*, *gpx*, *prxQ*, *cycP*, and *cpo*) encoding superoxide dismutase (SOD), catalase (CAT), and peroxidase (POD) (Fig. 4b and Table S3) were markedly increased, allowing the community to scavenge free radicals. Thioredoxin and thioredoxin reductase [48,49] are important defensive signaling molecules to maintain the cellular equilibrium of oxidation-reduction pertaining to cold stress. The abundances of four genes (*trxC*, *ybbN*, and *trxA-B*) encoding these proteins (Fig. 4b and Table S3) were also increased. The abundance of eight genes (*clpP*, *clpX*, *clpS*, *clpA-C*, *clpE*, and *clpL*) encoding the ATP-dependent Clp protease (Fig. 4b and Table S3) were also significantly augmented, which could aid the bacterial resistance to cold stress [50]. In general, the enrichment of these twenty-nine genes verifies that the microbial community was implementing a defensive response at low temperature.

The substrates for cellular proliferation (four nucleotides in Fig. S4) and energy cycle (five compounds related to the TCA cycle in Fig. S4) in microalgae at low temperature were not influenced by temperature variation; therefore, microalgae could play an important role in treating wastewater, complementing the bacterial community deficiency. More importantly, some microbial metabolic processes were upregulated to resist cold stress. For instance, the genes encoding the synthesis of trehalose and proline (*ostA-B*, *thuE*, and *thug*; *proV*, *proX*, *putA*, *pip*, *opuD*, and *prdF*), confirmed as storage compounds [51] and osmo-protectants [52] against cold stress were elevated (Fig. 4b and Table S3). The proline concentration at low temperature was 4.3- and 1.7-fold higher than at

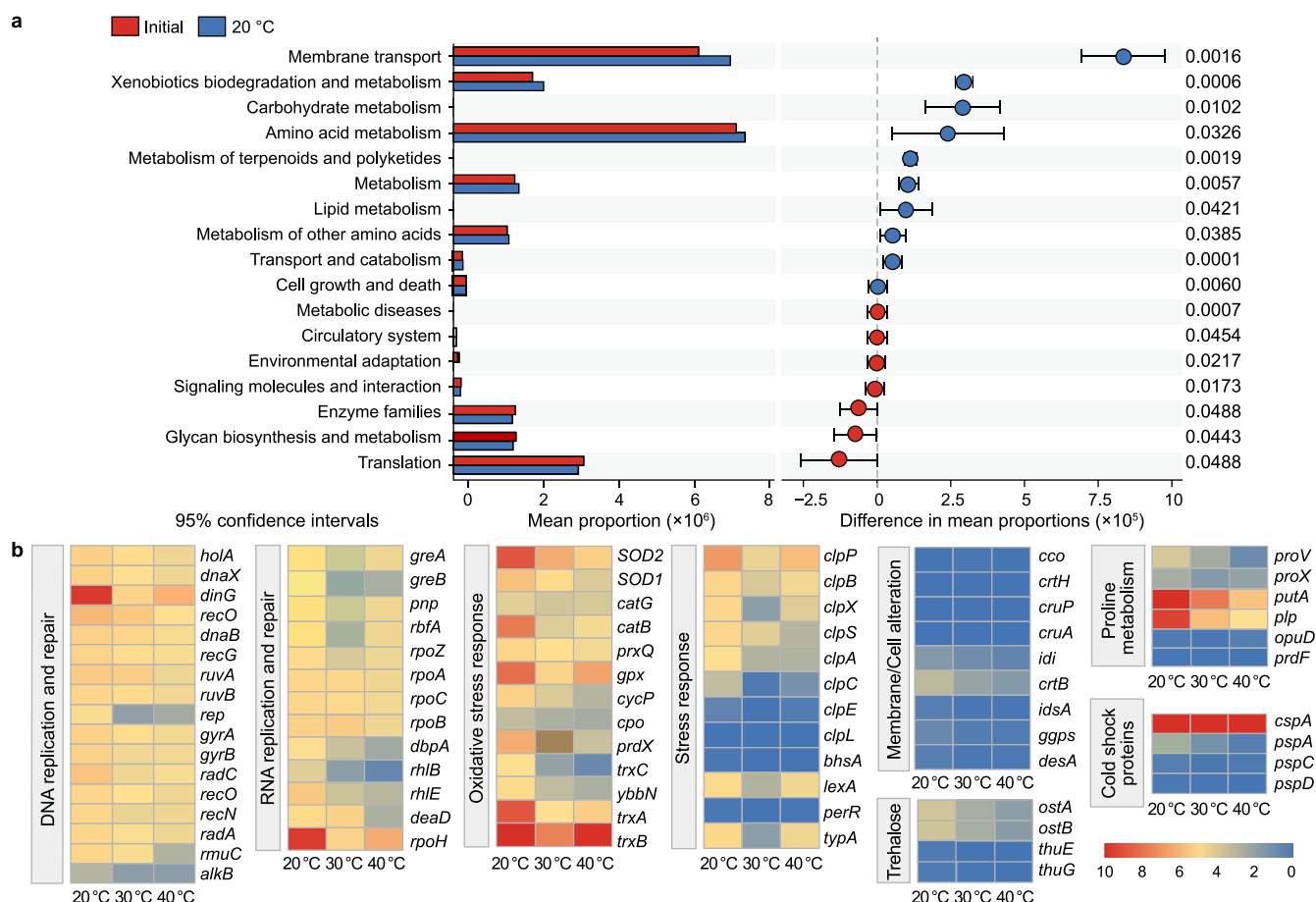


Fig. 4. Typical metabolic pathways (a) and key functional genes (b) of the microbial community in response to low temperature on day 2.

medium and high temperatures, respectively (Fig. S5). Additionally, the abundances of genes for altering membrane structure (*cco*, *crTH*, *cruP*, *cruA*, *idi*, *crtB*, *idsA*, *ggps*, and *desA*) and synthesis of related proteins (*greA-B*, *pnp*, *rbfA*, *rpoZ*, *rpoA-C*, *dbpA*, *rhlB*, *rhlE*, *deaD*, and *ropH*) (Fig. 4b and Table S3) were also increased. Overall, the metabolic mechanisms of the microbial community at low temperature showed a prominently defensive profile, which explained the declined cell growth and microbial abundance under this condition (Fig. 1).

3.2.3. Pivotal role of the microalgal ecological niche

In this study, the removal pattern of nutrients and the structure of the microbial community were markedly different from those in conventional activated sludge. Currently, the stochastic and deterministic processes are the two main patterns describing microbial community assembly [53]. Stochastic processes occur when the microbial community formation can be established based on overlooking the overlapping niches, even if the co-occurring competitive capacities are closely matched [54]. Conversely, deterministic processes illustrate that distinct niches are influenced by ecological selection [55]. The neutral community model is the prevalent method to evaluate the stochastic processes during the microbial community formation. When this was assessed, the resulting R^2 value was 0.499, revealing that most microorganisms were not determined by random drift because of the leading influence of microalgae. Therefore, the calculation of niche breadth and niche overlap was adopted to reveal the pivotal role of microalgal involvement.

After further modularizing the global co-occurrence network among the microbial community (Fig. S6), two obvious modules (16 nodes with blue background and 18 nodes with a red background, average clustering coefficient = 0.648) were determined to be the

core positive bacteria (Fig. 5b). The blue assemblages were mainly composed of heterotrophic bacteria involved in nitrogen removal (such as *Ralstonia* sp. and *Burkholderia* sp.), while the red assemblages were mainly involved in heterotrophic COD removal (such as *Bacillus* sp. and *Pseudomonas* sp.). Species with wider niche breadth are generalists because of the wide range of nutritional resources they can use [56]. After analysis, microalgae achieved the maximum niche breadth of 5.21 among these predominant bacterial species (Fig. 5c and the last yellow point in Fig. S7), further confirming that the microbial community niche response to temperature variation was predominated by microalgae. Additionally, niche overlap can describe function and resource competition among microbial species [10]. The average niche overlap in this biological system was 0.38 (dashed red line in Fig. 5d), illustrating reasonable reciprocity between eukaryotic microalgae and prokaryotic bacteria in terms of nutrient removal. The lower niche overlap sufficiently explained the lower α -diversity mentioned above (Table S1). The involvement of microalgae could trigger a deterministic distribution of the microbial community, making it suitable for advanced treatment. Assuring the predominance of the microalgal ecological niche could be the prerequisite to achieving preferable wastewater treatment efficiency when artificially constructing the MBC.

Additionally, the bacteria responsible for heterotrophic nitrogen removal under aerobic conditions, such as *B. intermedia* (the 7th point with a value of 0.13 in Fig. 5d) and *Burkholderiales multivorans* (the 9th point with a value of 0.22 in Fig. 5d), were below the average value of niche overlap. Accordingly, two exclusively characteristic phenomena appeared in the bacterial community during nitrogen metabolism. First, the abundance of most genes associated with nitrogen metabolism increased at medium temperature and declined at low temperature, indicating that microalgae play an

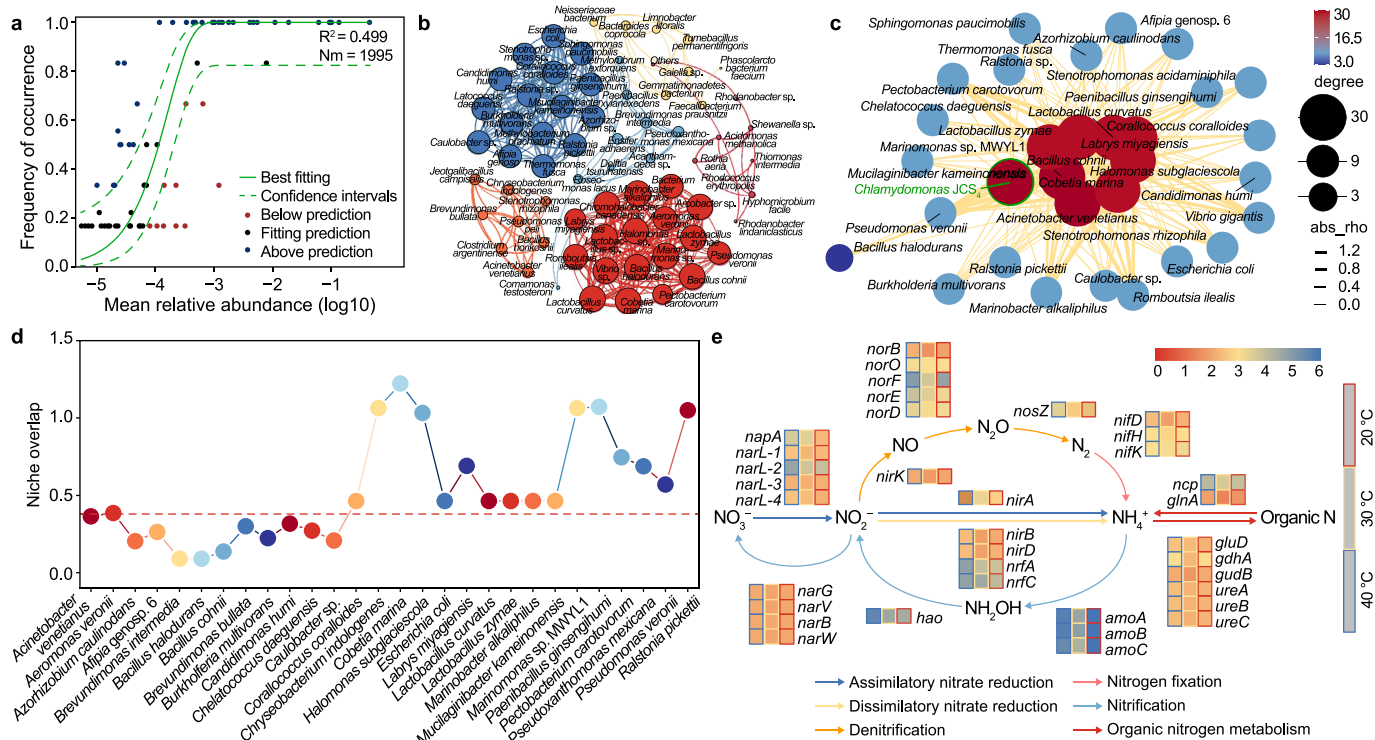


Fig. 5. a, Neutral community model of the bacterial community at different temperatures. b, Co-occurrence patterns of core bacterial taxa elicited by network analysis. Nodes are colored by taxonomy. c, Correlation interactions based on niche breadth calculation elicited by a network diagram. d, Profiles of niche overlap for predominant species compared with *Chlamydomonas* sp. J5C.4. e, Key functional genes involved in nitrogen metabolism at different temperatures.

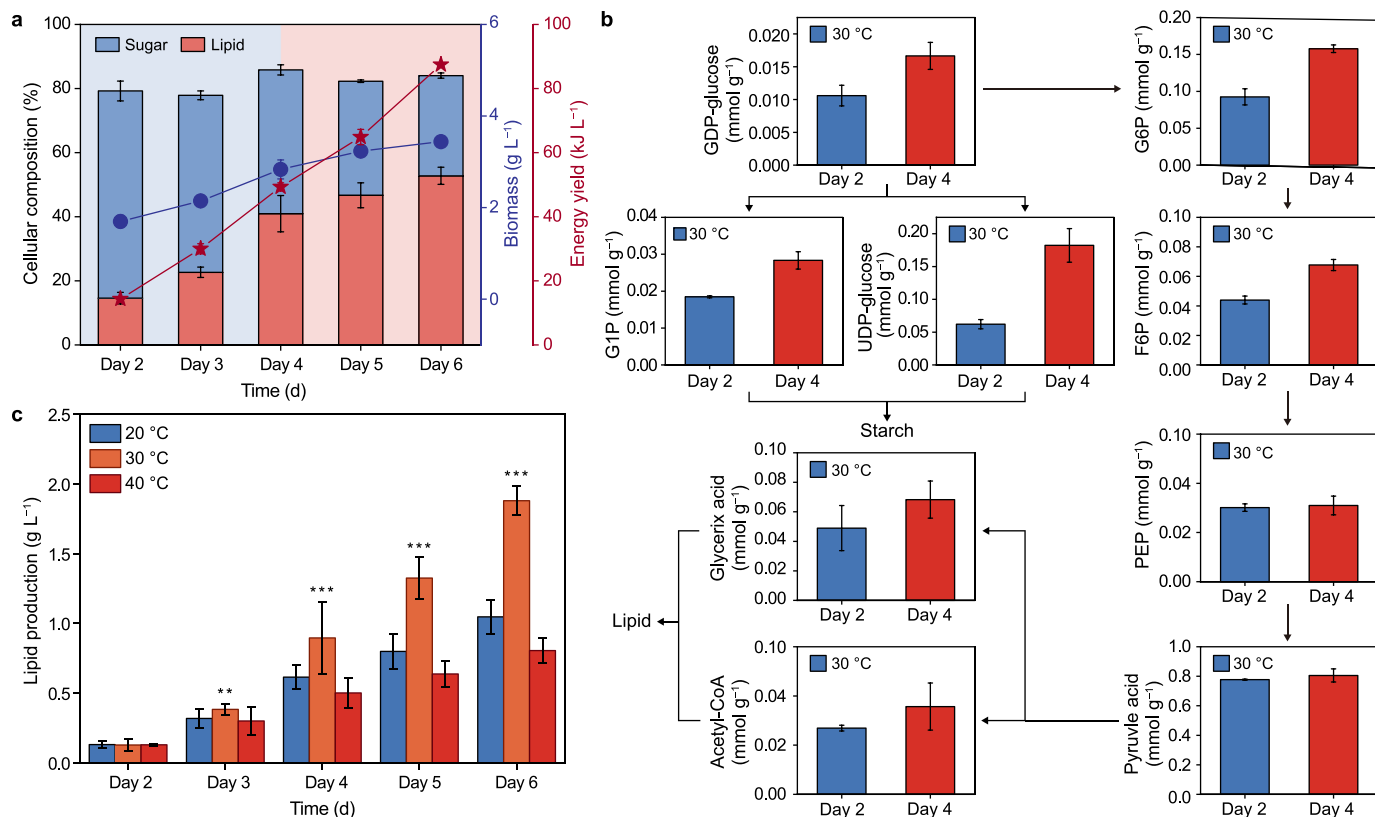


Fig. 6. a, Biomass, cellular composition, and energy yield at medium temperature. b, Metabolic profiling of microalgal energy-storage compounds at medium temperature. c, Microalgal lipid production at different temperatures. * $P < 0.05$, ** $P < 0.01$, and *** $P < 0.001$.

effective role in nitrogen removal at low temperature (Fig. 5e and Table S4). Second, the genes encoding nitrogen metabolism were detected with a disproportionate distribution.

For instance, the abundances of common genes associated with ammonia oxidation (*amoA-C* and *hao*) were the lowest (Fig. 5e), possibly because of the deficiency in the common autotrophic nitrifying bacteria (such as *Nitrosomonas* sp. and *Nitrosospira* sp.) [57]. However, the genes associated with nitrogen assimilation and organic metabolism (*hcp* and *glnA* for ammonia assimilation; *gluD*, *gdhA*, *gudB* and *ureA-C* for cellular organic nitrogen synthesis) and genes related to heterotrophic denitrification (*nirK* and *norB*) were most abundant (Fig. 5e), indicating nitrogen may be mainly removed through heterotrophic bacterial assimilation and denitrification [2].

3.3. Profiles of microalgal lipid and resource reclamation

Carbon sequestration and biomass bioenergy production are vital to achieving carbon neutrality [9]. In this study, the maximum energy yield was 87.4 kJ L⁻¹ at medium temperature on day 6 (Fig. 6a), which was 1.5- and 2.0-fold higher than that obtained at low and high temperatures, respectively (Fig. S8). An obvious shift of starch to lipid was observed, resulting in a 2.8-fold increase of lipid content from day 2–4 (blue block to red block in Fig. 6a). This could be verified from the corresponding metabolic profiling. At early stages, the metabolites associated with starch synthesis, such as guanosine diphosphate glucose (GDP-glucose), glucose-6-phosphate (G6P), fructose-6-phosphate (F6P), glucose-1-phosphate (G1P), and uridine-diphosphoglucose (UDP-glucose) were increased (Fig. 6b), indicating favorable carbon fixation (Fig. 3c). After that, primary metabolites correlated to lipid

biosynthesis such as phosphoenolpyruvate (PEP), pyruvic acid, glyceric acid, and acetyl coenzyme A (acetyl-CoA) increased until the end of the experiment (Fig. 6b). The most favorable biomass of 3.6 g L⁻¹ was achieved at medium temperature, contributing to a maximum lipid production of 1.9 g L⁻¹ on day 6 (Fig. 6c).

Microalgal biofuel could be an important renewable fuel for carbon-neutral energy systems [58]. The lipid production in this experiment at low temperature was 1.3-fold higher than that at high temperature, further confirming that this biological system is suitable for the advanced treatment of wastewater at low temperature (Fig. 6c). Additionally, the calculations of fatty acid composition to determine biodiesel quality, such as kinematic viscosity and cetane number, were in accordance with the requirements of European and United States standards (Fig. S9 and Table S5). This demonstrates that advanced treatment and resource reclamation could be achieved using a microalgae-bacteria niche wastewater treatment.

4. Conclusion

This study comprehensively demonstrated that an appropriate microalgae-bacteria niche treatment could result in flexible scenarios with similar biological functions through the enrichment of different dominant species in response to temperature variation. To our knowledge, this is the first study to corroborate the establishment of a bacterial community associated with microalgae by deterministic processes rather than stochastic processes. The niche breadth and niche overlap of microalgae in the microalgae-bacteria wastewater treatment were 5.21 and 0.38, respectively. At low temperature, microalgae contributed more to wastewater treatment to compensate for the cold stress experienced by the bacteria.

Moreover, heterotrophic bacteria capable of nitrogen removal were enriched with microalgae at medium and high temperatures. Pathogenic bacteria could be eliminated by microalgae photosynthesis. A satisfactory energy yield (87.4 kJ L^{-1}) and lipid production (1.9 g L^{-1}) were achieved at medium temperature, indicating both advanced wastewater treatment and resource reclamation could be achieved using this method.

Declaration of competing interest

The authors declare that they have no known competing financial interests or personal relationships that could have appeared to influence the work reported in this paper.

Acknowledgments

This work was financially supported by the National Key Research and Development Program (No. 2019YFC0408503) and Fund Project of National and Local Joint Engineering Research Center for Biomass Energy Development and Utilization (Harbin Institute of Technology, Project No. 2021A004).

Appendix A. Supplementary data

Supplementary data to this article can be found online at <https://doi.org/10.1016/j.ese.2022.100230>.

References

- [1] E. Díaz, L. Pintado, L. Faba, S. Ordóñez, J.M. González-LaFuente, Effect of sewage sludge composition on the susceptibility to spontaneous combustion, *J. Hazard Mater.* 361 (2019) 267–272, <https://doi.org/10.1016/j.jhazmat.2018.08.094>.
- [2] Y. Peng, S. He, F. Wu, Biochemical processes mediated by iron-based materials in water treatment: enhancing nitrogen and phosphorus removal in low C/N ratio wastewater, *Sci. Total Environ.* 775 (2021), 145137, <https://doi.org/10.1016/j.scitotenv.2021.145137>.
- [3] R.K. Goswami, K. Agrawal, P. Verma, Multifaceted role of microalgae for municipal wastewater treatment: a futuristic outlook toward wastewater management, *Clean: Soil, Air, Water* (2022), 2100286, <https://doi.org/10.1002/clen.202100286>.
- [4] S.S. Chan, K.S. Khoo, K.W. Chew, T.C. Ling, P.L. Show, Recent advances biodegradation and biosorption of organic compounds from wastewater: microalgae-bacteria consortium - a review, *Bioresour. Technol.* 344 (2022), 126159, <https://doi.org/10.1016/j.biortech.2021.126159>.
- [5] G.Y. Yew, B.K. Puah, K.W. Chew, S.Y. Teng, P.L. Show, T.H.P. Nguyen, *Chlorella vulgaris* FSP-E cultivation in waste molasses: photo-to-property estimation by artificial intelligence, *Chem. Eng. J.* 402 (2020), 126230, <https://doi.org/10.1016/j.cej.2020.126230>.
- [6] X. You, L. Yang, X. Zhou, Y. Zhang, Sustainability and carbon neutrality trends for microalgae-based wastewater treatment: a review, *Environ. Res.* 209 (2022), 112860, <https://doi.org/10.1016/j.envres.2022.112860>.
- [7] R.K. Oruganti, K. Katam, P.L. Show, V. Gadhamshetty, V.K.K. Upadhyayula, D. Bhattacharyya, A comprehensive review on the use of algal-bacterial systems for wastewater treatment with emphasis on nutrient and micropollutant removal, *Bioengineered* 13 (4) (2022) 10412–10453, <https://doi.org/10.1080/21655979.2022.2056823>.
- [8] C. Zhang, S. Li, S.H. Ho, Converting nitrogen and phosphorus wastewater into bioenergy using microalgae-bacteria consortia: a critical review, *Bioresour. Technol.* 342 (2021b), 126056, <https://doi.org/10.1016/j.biortech.2021.126056>.
- [9] F. Wang, J.D. Harindintwali, Z. Yuan, M. Wang, F. Wang, S. Li, Z. Yin, L. Huang, Y. Fu, L. Li, S.X. Chang, L. Zhang, J. Rinklebe, Z. Yuan, Q. Zhu, L. Xiang, D.C.W. Tsang, L. Xu, X. Jiang, J. Liu, N. Wei, M. Kästner, Y. Zou, Y.S. Ok, J. Shen, D. Peng, W. Zhang, D. Barceló, Y. Zhou, Z. Bai, B. Li, B. Zhang, K. Wei, H. Cao, Z. Tan, L.B. Zhao, X. He, J. Zheng, N. Bolan, X. Liu, C. Huang, S. Dietmann, M. Luo, N. Sun, J. Gong, Y. Gong, F. Brahusli, T. Zhang, C. Xiao, X. Li, W. Chen, N. Jiao, J. Lehmann, Y.G. Zhu, H. Jin, A. Schäffer, J.M. Tiedje, J.M. Chen, Technologies and perspectives for achieving carbon neutrality, *Innovation* 2 (4) (2021a), 100180, <https://doi.org/10.1016/j.xinn.2021.100180>.
- [10] N. Li, W. Zeng, Y. Guo, C. Li, C. Ma, Y. Peng, Nitrogen-associated niche characteristics and bacterial community estimated by ^{15}N -DNA-stable isotope probing in one-stage partial nitrification/anammox process with different ammonium loading, *J. Environ. Manag.* 247 (2019b) 603–612, <https://doi.org/10.1016/j.jenvman.2019.06.110>.
- [11] N. Wang, J. Gao, Y. Liu, Q. Wang, X. Zhuang, G. Zhuang, Realizing the role of N-acyl-homoserine lactone-mediated quorum sensing in nitrification and denitrification: a review, *Chemosphere* 274 (2021b), 129970, <https://doi.org/10.1016/j.chemosphere.2021.129970>.
- [12] W. Liu, Y. Wu, S. Zhang, Y. Gao, Y. Jiang, H. Horn, J. Li, Successful granulation and microbial differentiation of activated sludge in anaerobic/anoxic/aerobic (A^2O) reactor with two-zone sedimentation tank treating municipal sewage, *Water Res.* 178 (2020), 115825, <https://doi.org/10.1016/j.watres.2020.115825>.
- [13] F. Yang, C. Zhang, H. Rong, Y. Cao, Research progress and application prospect of anaerobic biological phosphorus removal, *Appl. Microbiol. Biotechnol.* 103 (5) (2019) 2133–2139, <https://doi.org/10.1007/s00253-019-09634-0>.
- [14] N.S. Mat Aron, K.S. Khoo, K.W. Chew, A. Veeramuthu, J.S. Chang, P.L. Show, Microalgae cultivation in wastewater and potential processing strategies using solvent and membrane separation technologies, *J. Water Proc. Eng.* 39 (2021), 101701, <https://doi.org/10.1016/j.jpwe.2020.101701>.
- [15] K.S. Khoo, W.Y. Chia, K.W. Chew, P.L. Show, Microalgal-bacterial consortia as future prospect in wastewater bioremediation, environmental management and bioenergy production, *Indian J. Microbiol.* 61 (3) (2021) 262–269, <https://doi.org/10.1007/s12088-021-00924-8>.
- [16] C. Zhang, T. Hasunuma, S. Shiung Lam, A. Kondo, S.H. Ho, Salinity-induced microalgal-based mariculture wastewater treatment combined with biodiesel production, *Bioresour. Technol.* 340 (2021a), 125638, <https://doi.org/10.1016/j.biortech.2021.125638>.
- [17] W. Qu, C. Zhang, Y. Zhang, S.H. Ho, Optimizing real swine wastewater treatment with maximum carbohydrate production by a newly isolated indigenous microalgae *Parachlorella kessleri* QWY28, *Bioresour. Technol.* 289 (2019), 121702, <https://doi.org/10.1016/j.biortech.2019.121702>.
- [18] S.H. Ho, A. Nakanishi, X. Ye, J.S. Chang, C.Y. Chen, T. Hasunuma, A. Kondo, Dynamic metabolic profiling of the marine microalgae *Chlamydomonas* sp. JSC4 and enhancing its oil production by optimizing light intensity, *Biotechnol. Biofuels* 8 (1) (2015) 48, <https://doi.org/10.1186/s13068-015-0226-y>.
- [19] H. Feng, C. Sun, C. Zhang, H. Chang, N. Zhong, W. Wu, H. Wu, X. Tan, M. Zhang, S.H. Ho, Bioconversion of mature landfill leachate into biohydrogen and volatile fatty acids via microalgal photosynthesis together with dark fermentation, *Energy Convers. Manag.* (2021), 115035, <https://doi.org/10.1016/j.enconman.2021.115035>.
- [20] W. Mohr Philip, S. Krawiec, Temperature characteristics and Arrhenius plots for nominal psychrophiles, mesophiles and thermophiles, *J. Gen. Microbiol.* 121 (2) (1980) 311–317, <https://doi.org/10.1099/00221287-121-2-311>.
- [21] W.T. Sloan, M. Lunn, S. Woodcock, I.M. Head, S. Nee, T.P. Curtis, Quantifying the roles of immigration and chance in shaping prokaryote community structure, *Environ. Microbiol.* 8 (2006) 732–740, <https://doi.org/10.1111/j.1462-2920.2005.00956.x>.
- [22] J. Yu, S.N. Tang, P.K.H. Lee, Microbial communities in full-scale wastewater treatment systems exhibit deterministic assembly processes and functional dependency over time, *Environ. Sci. Technol.* 55 (8) (2021) 5312–5323, <https://doi.org/10.1021/acs.est.0c06732>.
- [23] K. Wisniewski, M. Kowalski, J. Makinia, Modeling nitrous oxide production by a denitrifying-enhanced biologically phosphorus removing (EBPR) activated sludge in the presence of different carbon sources and electron acceptors, *Water Res.* 142 (2018) 55–64, <https://doi.org/10.1016/j.watres.2018.05.041>.
- [24] L. Zhang, Z. Shen, W.K. Fang, G. Gao, Composition of bacterial communities in municipal wastewater treatment plant, *Sci. Total Environ.* 689 (2019) 1181–1191, <https://doi.org/10.1016/j.scitotenv.2019.06.432>.
- [25] Y. Fan, J. Chen, G. Shirkey, R. John, S.R. Wu, H. Park, C. Shao, Applications of structural equation modeling (SEM) in ecological studies: an updated review, *Ecol. Processes* 5 (1) (2016) 19, <https://doi.org/10.1186/s13717-016-0063-3>.
- [26] K.D. Young, Bacterial morphology: why have different shapes? *Curr. Opin. Microbiol.* 10 (6) (2007) 596–600, <https://doi.org/10.1016/j.mib.2007.09.009>.
- [27] K. Li, Q. Liu, F. Fang, R. Luo, Q. Lu, W. Zhou, S. Huo, P. Cheng, J. Liu, M. Addy, P. Chen, D. Chen, R. Ruan, Microalgae-based wastewater treatment for nutrients recovery: a review, *Bioresour. Technol.* 291 (2019a), 121934, <https://doi.org/10.1016/j.biortech.2019.121934>.
- [28] H.J. de Vries, A.J.M. Stams, C.M. Plugge, Biodiversity and ecology of microorganisms in high pressure membrane filtration systems, *Water Res.* 172 (2020), 115511, <https://doi.org/10.1016/j.watres.2020.115511>.
- [29] H. Zhou, X. Li, G. Xu, H. Yu, Overview of strategies for enhanced treatment of municipal/domestic wastewater at low temperature, *Sci. Total Environ.* 643 (2018) 225–237, <https://doi.org/10.1016/j.scitotenv.2018.06.100>.
- [30] V. Kapoor, M. Elk, X. Li, J.W. Santo Domingo, Inhibitory effect of cyanide on wastewater nitrification determined using SOUR and RNA-based gene-specific assays, *Lett. Appl. Microbiol.* 63 (2) (2016) 155–161, <https://doi.org/10.1111/lam.12603>.
- [31] Y. Chen, Y. Zhang, L. Zhang, S. Zhang, Y. Peng, Applicability of two-stage anoxic/oxic shortcut nitrogen removal via partial nitrification and partial denitrification for municipal wastewater by adding sludge fermentation products continuously, *Chemosphere* 287 (2022), 132053, <https://doi.org/10.1016/j.chemosphere.2021.132053>.
- [32] M. Proszkowiec-Weglarz, K.B. Miska, L.L. Schreier, C.J. Grim, K.G. Jarvis, J. Shao, S. Vaessen, R. Sygall, M.C. Jenkins, S. Kahl, B. Russell, Research Note: effect of butyric acid glycerol esters on ileal and cecal mucosal and luminal microbiota in chickens challenged with *Eimeria maxima*, *Poultry Sci.* 99 (10) (2020) 5143–5148, <https://doi.org/10.1016/j.psj.2020.06.022>.
- [33] R.E. Beattie, T. Skwor, K.R. Hristova, Survivor microbial populations in post-chlorinated wastewater are strongly associated with untreated hospital sewage and include ceftazidime and meropenem resistant populations, *Sci.*

- Total Environ. 740 (2020), 140186, <https://doi.org/10.1016/j.scitotenv.2020.140186>.
- [34] S. Liu, G.G. Ying, Y.S. Liu, F.Q. Peng, L.Y. He, Degradation of norgestrel by bacteria from activated sludge: comparison to progesterone, Environ. Sci. Technol. 47 (18) (2013) 10266–10276, <https://doi.org/10.1021/es304688g>.
- [35] C.L. Amorim, A.S. Maia, R.B.R. Mesquita, A.O.S.S. Rangel, M.C.M. van Loosdrecht, M.E. Tiritan, P.M.L. Castro, Performance of aerobic granular sludge in a sequencing batch bioreactor exposed to ofloxacin, norfloxacin and ciprofloxacin, Water Res. 50 (2014) 101–113, <https://doi.org/10.1016/j.watres.2013.10.043>.
- [36] T. He, J. Bao, Y. Leng, D. Snow, S. Kong, T. Wang, X. Li, Biotransformation of doxycycline by *Brevundimonas naejangsansensis* and *Sphingobacterium mizutaii* strains, J. Hazard Mater. 411 (2021), 125126, <https://doi.org/10.1016/j.jhazmat.2021.125126>.
- [37] W.S. Chai, W.G. Tan, H.S. Halimatul Munawaroh, V.K. Gupta, S.H. Ho, P.L. Show, Multifaceted roles of microalgae in the application of wastewater biotreatment: a review, Environ. Pollut. 269 (2021), 116236, <https://doi.org/10.1016/j.envpol.2020.116236>.
- [38] A.P. Peter, K.S. Khoo, K.W. Chew, T.C. Ling, S.H. Ho, J.S. Chang, P.L. Show, Microalgae for biofuels, wastewater treatment and environmental monitoring, Environ. Chem. Lett. 19 (2021) 2891–2904, <https://doi.org/10.1007/s10311-021-01219-6>.
- [39] P.K. Arora, *Bacilli*-Mediated degradation of xenobiotic compounds and heavy metals, Front. Bioeng. Biotechnol. 8 (2020) 1100, <https://doi.org/10.3389/fbioe.2020.570307>.
- [40] C.Y. Chen, S.H. Yen, Y.C. Chung, Combination of photoreactor and packed bed bioreactor for the removal of ethyl violet from wastewater, Chemosphere 117 (2014) 494–501, <https://doi.org/10.1016/j.chemosphere.2014.08.069>.
- [41] A. Tabernacka, E. Zborowska, K. Pogoda, M. Zoladek, Removal of tetrachloroethene from polluted air by activated sludge, Environ. Technol. 40 (4) (2019) 470–479, <https://doi.org/10.1080/09593330.2017.1397759>.
- [42] N.C.S. Mykytczuk, S.J. Foote, C.R. Omelon, G. Southam, C.W. Greer, L.G. Whyte, Bacterial growth at -15 °C; molecular insights from the permafrost bacterium *Planococcus halocryophilus* Or1, ISME J. 7 (6) (2013) 1211–1226, <https://doi.org/10.1038/ismej.2013.8>.
- [43] J.M. Xia, X.M. Hu, C.H. Huang, L.B. Yu, R.F. Xu, X.X. Tang, D.H. Lin, Metabolic profiling of cold adaptation of a deep-sea psychrotolerant Microbacterium sediminis to prolonged low temperature under high hydrostatic pressure, Appl. Microbiol. Biotechnol. 104 (1) (2020) 277–289, <https://doi.org/10.1007/s00253-019-10134-4>.
- [44] C.L. Yao, G.N. Somero, Thermal stress and cellular signaling processes in hemocytes of native (*Mytilus californianus*) and invasive (*M. galloprovincialis*) mussels: cell cycle regulation and DNA repair, Comp. Biochem. Physiol. Mol. Integr. Physiol. 165 (2) (2013) 159–168, <https://doi.org/10.1016/j.cbpa.2013.02.024>.
- [45] S. Kumar, D.C. Suyal, A. Yadav, Y. Shouche, R. Goel, Psychrophilic *Pseudomonas helmanticensis* proteome under simulated cold stress, Cell Stress Chaperones 25 (6) (2020) 1025–1032, <https://doi.org/10.1007/s12192-020-01139-4>.
- [46] G. Horn, R. Hofweber, W. Kremer, H.R. Kalbitzer, Structure and function of bacterial cold shock proteins, Cell. Mol. Life Sci. 64 (12) (2007) 1457, <https://doi.org/10.1007/s00018-007-6388-4>.
- [47] L. Zhang, X. Wang, M. Yu, Y. Qiao, X.H. Zhang, Genomic analysis of *Luteimonas abyssi* XH031T: insights into its adaption to the subseafloor environment of South Pacific Gyre and ecological role in biogeochemical cycle, BMC Genom. 16 (1) (2015) 1092, <https://doi.org/10.1186/s12864-015-2326-2>.
- [48] S.S. Kazemi-Shahandashti, R. Maali-Amiri, Global insights of protein responses to cold stress in plants: signaling, defence, and degradation, J. Plant Physiol. 226 (2018) 123–135, <https://doi.org/10.1016/j.jplph.2018.03.022>.
- [49] M. Serata, T. Iino, E. Yasuda, T. Sako, Roles of thioredoxin and thioredoxin reductase in the resistance to oxidative stress in *Lactobacillus casei*, Microbiology 158 (4) (2012) 953–962, <https://doi.org/10.1099/mic.0.053942-0>.
- [50] S. Roy, Y. Zhu, J. Ma, A.C. Roy, Y. Zhang, X. Zhong, Z. Pan, H. Yao, Role of ClpX and ClpP in *Streptococcus suis* serotype 2 stress tolerance and virulence, Microbiol. Res. 223–225 (2019) 99–109, <https://doi.org/10.1016/j.micres.2019.04.003>.
- [51] M. Vanaporn, R.W. Titball, Trehalose and bacterial virulence, Virulence 11 (1) (2020) 1192–1202, <https://doi.org/10.1080/21505594.2020.1809326>.
- [52] M. Zubair, A. Hanif, A. Farzand, T.M. Sheikh, A.R. Khan, M. Suleman, M. Ayaz, X. Gao, Genetic screening and expression analysis of psychrophilic *Bacillus* spp. reveal their potential to alleviate cold stress and modulate phytohormones in wheat, Microorganisms 7 (9) (2019), <https://doi.org/10.3390/microorganisms7090337>.
- [53] S. Jiao, Y.f. Yang, Y.Q. Xu, J. Zhang, Y.H. Lu, Balance between community assembly processes mediates species coexistence in agricultural soil microbiomes across eastern China, ISME J. 14 (1) (2020) 202–216, <https://doi.org/10.1038/s41396-019-0522-9>.
- [54] J.C. Stegen, X.J. Lin, A.E. Konopka, J.K. Fredrickson, Stochastic and deterministic assembly processes in subsurface microbial communities, ISME J. 6 (9) (2012) 1653–1664, <https://doi.org/10.1038/ismej.2012.22>.
- [55] F. Dini-Andreote, J.C. Stegen, J.D. van Elsland, J.F. Salles, Disentangling mechanisms that mediate the balance between stochastic and deterministic processes in microbial succession, Proc. Natl. Acad. Sci. U.S.A. 112 (2015) 1326–1332, <https://doi.org/10.1073/pnas.1414261112>.
- [56] E.E.L. Muller, N. Pinel, C.C. Laczny, M.R. Hoopmann, S. Narayanasamy, L.A. Lebrun, H. Roume, J. Lin, P. May, N.D. Hicks, A. Heintz-Buschart, L. Wampach, C.M. Liu, L.B. Price, J.D. Gillece, C. Guignard, J.M. Schupp, N. Vlassis, N.S. Baliga, R.L. Moritz, P.S. Keim, P. Wilmes, Community-integrated omics links dominance of a microbial generalist to fine-tuned resource usage, Nat. Commun. 5 (1) (2014) 5603, <https://doi.org/10.1038/ncomms6603>.
- [57] A. Terada, S. Lackner, K. Kristensen, B.F. Smets, Inoculum effects on community composition and nitrification performance of autotrophic nitrifying biofilm reactors with counter-diffusion geometry, Environ. Microbiol. 12 (10) (2010) 2858–2872, <https://doi.org/10.1111/j.1462-2920.2010.02267.x>.
- [58] D. Nagarajan, J.S. Chang, D.J. Lee, Pretreatment of microalgal biomass for efficient biohydrogen production - recent insights and future perspectives, Bioresour. Technol. 302 (2020), 122871, <https://doi.org/10.1016/j.biortech.2020.122871>.